



Proceeding Paper

Non-Invasive Disease Stage Classification of Bitter Rot in Fruits Using Optical Coherence Tomography and Intensity-Based Image Analysis †

Amila Dhanushka Karunanayaka ¹, Nipun Shantha Kahatapitiya ², Nisala Damith ³, Jeehyun Kim ², Mansik Jeon ², Bhagya Nathali Silva ^{4,5}, Ruchire Eranga Wijesinghe ^{1,5,*} and Udaya Wijenayake ^{3,*}

- Department of Electrical and Electronic Engineering, Faculty of Engineering, Sri Lanka Institute of Information Technology, Malabe 10115, Sri Lanka; karunanayakaamila197@gmail.com (A.D.K.)
- ² School of Electronic and Electrical Engineering, College of IT Engineering, Kyungpook National University, Daegu 41566, Republic of Korea; nipunshantha@knu.ac.kr (N.S.K.); jeehk@knu.ac.kr (J.K.); msjeon@knu.ac.kr (M.J.)
- Department of Computer Engineering, Faculty of Engineering, University of Sri Jayewardenepura, Nugegoda 10250, Sri Lanka; en93909@sjp.ac.lk (N.D.)
- Department of Information Technology, Faculty of Computing, Sri Lanka Institute of Information Technology, Malabe 10115, Sri Lanka; nathali.s@sliit.lk (B.N.S.)
- ⁵ Center for Excellence in Informatics, Electronics and Transmission (CIET), Sri Lanka Institute of Information Technology, Malabe 10115, Sri Lanka
- * Correspondence: eranga.w@sliit.lk (R.E.W.); udayaw@sjp.ac.lk (U.W.)
- [†] Presented at the 12th International Electronic Conference on Sensors and Applications (ECSA-12), 12–14 November 2025; Available online: https://sciforum.net/event/ECSA-12.

Abstract

Plant disease has a tremendous impact on global food security, and *Colletotrichum* spp. caused bitter rot is a greater challenge to post-harvest quality. Conventional diagnosis is precise but invasive and therefore inappropriate for real-time purposes. This study investigates optical coherence tomography (OCT) as a high-resolution, non-invasive imaging method to detect internal structural changes from disease progression. The developed OCT-based image analysis framework stages diseases by assessing morphological degradation. The discovery of unique oval-shaped internal features, invisible to other non-invasive methods, demonstrates OCT's potential for early detection, accurate monitoring, and real-time application in precision agriculture.

Keywords: optical coherence tomography (OCT); bitter rot; non-invasive imaging; post-harvest disease detection; morphological degradation; disease staging; precision agriculture

Academic Editor(s): Name

Published: date

Citation: Karunanayaka, A.D.; Kahatapitiya, N.S.; Damith, N.; Kim, J.; Jeon, M.; Silva, B.N.; Wijesinghe, R.E.; Wijenayake, U. Non-Invasive Disease Stage Classification of Bitter Rot in Fruits Using Optical Coherence Tomography and Intensity-Based Image Analysis. *Eng. Proc.* 2025, volume number, x. https://doi.org/10.3390/xxxxx

Copyright: © 2025 by the authors. Submitted for possible open access publication under the terms and conditions of the Creative Commons Attribution (CC BY) license (https://creativecommons.org/license s/by/4.0/).

1. Introduction

Biophotonic innovation in medical and agricultural engineering has necessitated the quest to develop non-invasive methods to probe biological materials more accurately. *Colletotrichum* spp. causing bitter rot is one of the most severe diseases of cultivation and post-harvest storage of many fruits, including apples [1]. Symptoms begin as small gray or brown spots that develop in a concentric pattern from the infection site, eventually causing extensive tissue damage [2]. Despite the use of fungicides and optimized storage

Eng. Proc. 2025, x, x https://doi.org/10.3390/xxxxx

conditions to manage the disease, its early stages remain poorly understood; therefore, a specific non-invasive detection technique is required [1].

Traditional diagnostic techniques, such as histological examination and polymerase chain reaction (PCR), although precise, are time-consuming, invasive, and therefore less suitable for real-time surveillance [3–6]. Non-destructive analysis techniques such as visual examination, magnetic resonance imaging (MRI), X-rays, positron emission tomography (PET), confocal microscopy, fluorescence spectroscopy, and near infra-red (NIR) spectroscopy often have low resolution, long processing times, and limited depth penetration, making them less suitable for application in agriculture [7–9].

OCT has been a promising technique to study structural characteristics with micrometer-level resolution owing to its non-contact nature and depth-resolved imaging capability [10–12]. This study focuses on exploring the potential of OCT for the identification and monitoring of bitter rot disease development in fruits. By providing high-resolution, depth-resolved imaging with enhanced optical sensitivity, OCT offers the ability to accurately characterize morphological changes associated with disease progression. The technique's capability to visualize internal tissue structures at the micrometer scale presents opportunities for investigating degradation patterns in both depth and lateral dimensions. This research aims to establish OCT as a novel non-invasive tool for the early detection and management of bitter rot infection in various fruits, contributing to improved strategies in agricultural disease diagnosis and control.

2. Materials and Experimental Procedures

2.1. Swept-Source OCT System Configuration

A laboratory customized swept-source OCT (SS-OCT) system, shown in Figure 1, was used for image acquisition. The OCT system consists of a 1310 nm laser (Axsun Technologies, USA) with a 12 mm coherence length, 110 nm sweep bandwidth, 20 mW output power, and 100 kHz sweep rate [13]. A 50:50 optical fiber coupler (Gooch & Housego, UK) split the light between the sample and reference arms. The signals were detected using a balanced photodetector (Thorlabs, USA) and digitized via a 12-bit waveform digitizer (Alazar Technologies Inc., Canada). Processed signals generated OCT images over a 4 mm \times 4 mm scan area, calibrated using a refractive index of 1.42. The system achieved axial and lateral resolutions of 7.5 μ m and 10 μ m in air, and 7 μ m in plant tissues, as described in [13].

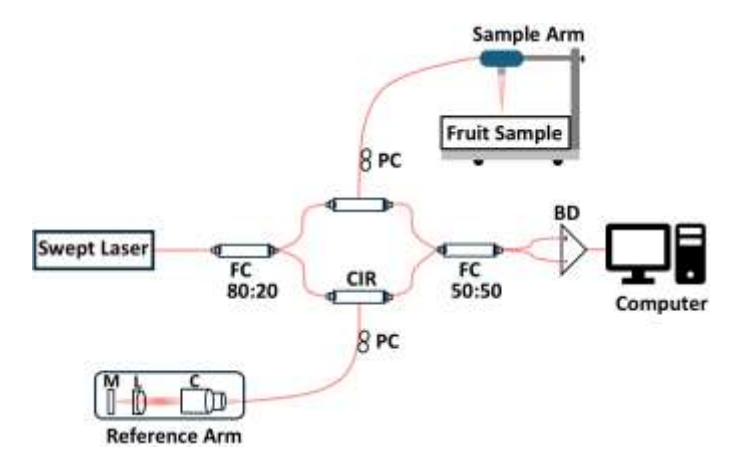


Figure 1. System architecture of the swept-source OCT (SS-OCT) setup. Abbreviations: BD—Balanced Detector; C—Collimator; CIR—Circulator; FC—Fiber coupler; L—Lens; M—Mirror; OL—Objective lens; PC—Polarization controller.

2.2. Signal Analysis and Data Processing

Assessment of tissue structure via OCT signal changes along axial and lateral dimensions was performed using a standard refractive index of 1.42 for plant cells [13]. Although tissues have unique refractive indices, this value streamlined analysis. A laboratory customized MATLAB (Math works, USA) program was implemented to generate intensity profiles by averaging pixel values row-wise (lateral) and column-wise (axial) within the region of interest (ROI) as shown in Figure S1 [14]. This method enabled effective quantification and visualization of internal structural changes in the specimens.

2.3. Analysis of Disease Progression and Boundary Detection

Beyond depth-based OCT analysis, this study examined the temporal progression of infected tissue thickness in the epidermis and hypodermis layers (Figure 2a). Canny edge detection was used to segment diseased regions, enabling focused analysis by excluding healthy areas [15]. A MATLAB script then mapped these boundaries spatially over time (Figure 2b), quantifying lateral infection spread. This method offered precise insight into the spatial and temporal dynamics of bitter rot progression within tissue layers.

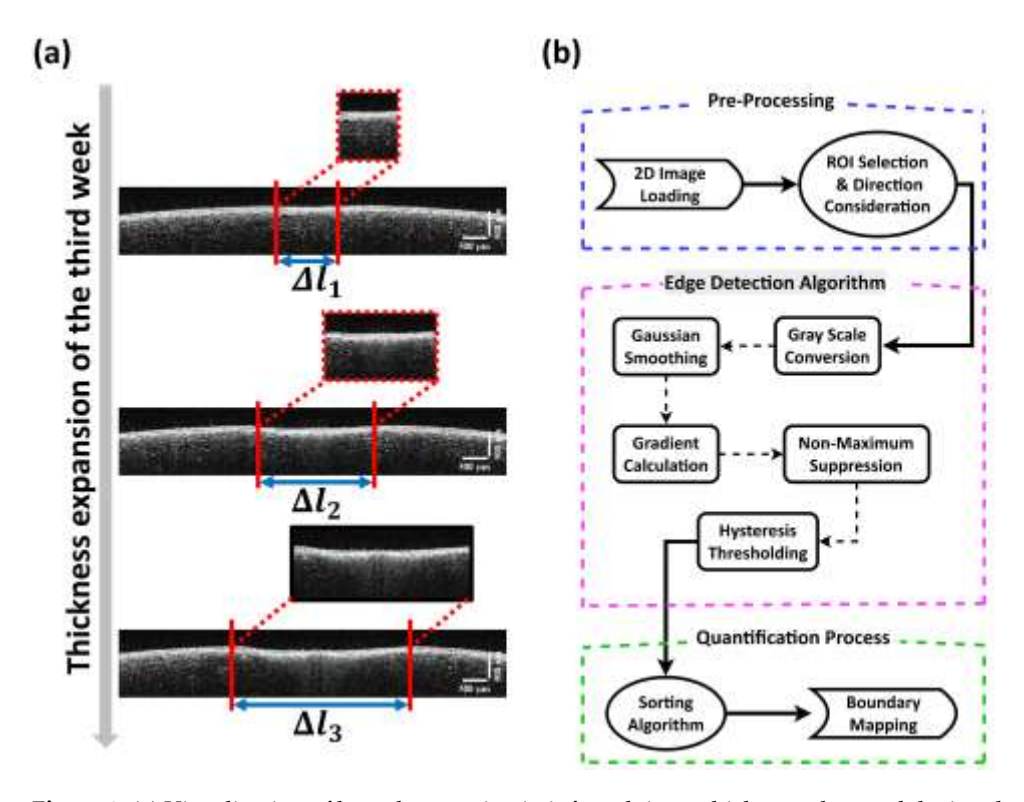


Figure 2. (a) Visualization of lateral expansion in infected tissue thickness observed during the third week of disease progression; (b) Flowchart illustrates the key steps in the boundary detection method used to identify infected regions. Δl_1 , Δl_2 , and Δl_3 indicate the measured thickness expansion over third week.

3. Results

3.1. Dynamic Thickness Profiling

A customized MATLAB-based algorithm was developed to monitor tissue degradation in third-week OCT data. From the initial inspection, nine two-dimensional (2D) OCT images showing potential infection were selected for detailed analysis (Figure 3a). A fixed 30 × 465-pixel region was scanned in each 2D OCT image to track lateral disease progression. The processing pipeline included Gaussian smoothing, gradient calculation, and edge detection, followed by a sorting-based method for accurate boundary mapping.

Infected regions were automatically highlighted (Figure 3b–j), and lateral thickness expansion was quantified and plotted (Figure 3k). This approach enables a comprehensive, non-invasive visual and quantitative assessment of infection spread during third week.

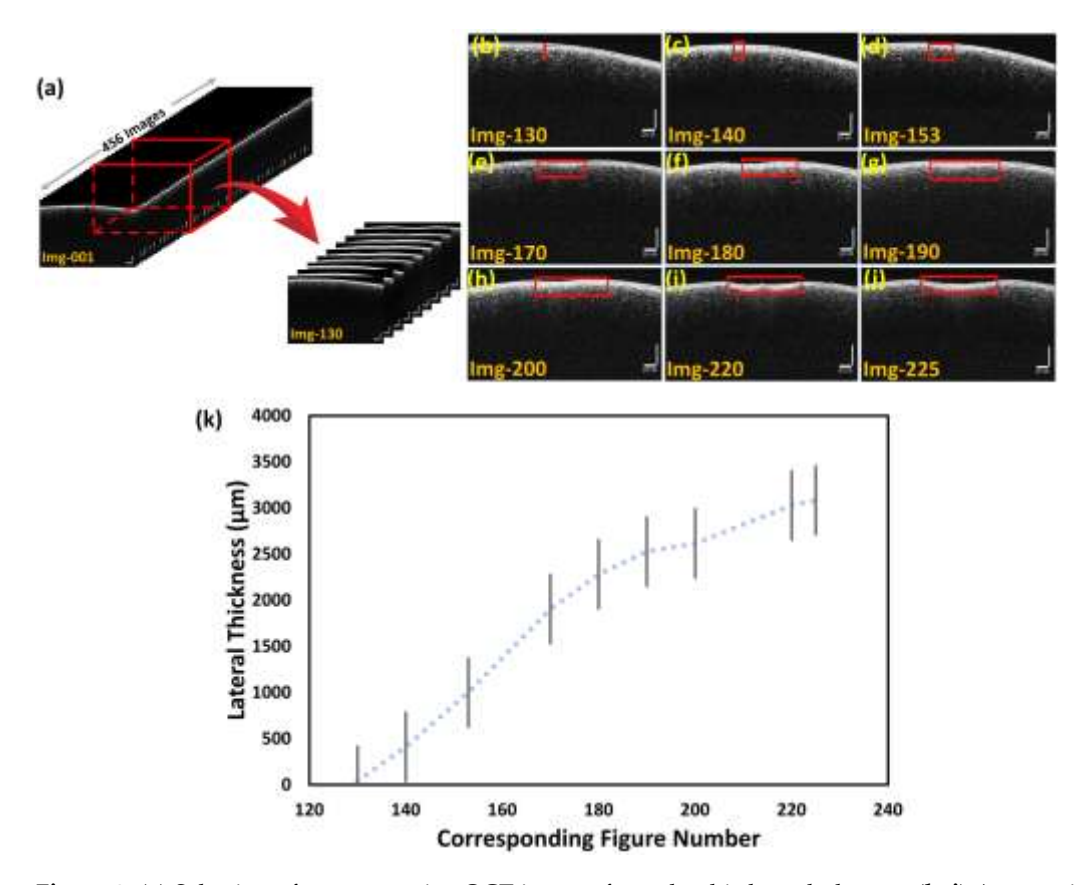


Figure 3. (a) Selection of representative OCT images from the third-week dataset; (b–j) Automatically detected and highlighted tissue degradation regions using the developed MATLAB algorithm; (k) Quantified lateral thickness expansion of the infected regions across selected third-week images.

3.2. Layer Distortion Along Depth Direction

To further analyze the disease progression, a MATLAB program was developed, which quantifies the structural degradation from bitter rot using OCT imaging. A 125 \times 350-pixel region was examined across OCT images representing healthy-infected, partially healthy, and fully infected tissues from weeks 1, 5, and 7. Averaged axial intensity profiles were computed to evaluate subsurface structural disruption. These profiles revealed progressive degradation, with clear layer-wise breakdown in advanced infection stages. As shown in Figure 4, axial profiling effectively captures microstructural changes, demonstrating OCT's strength in characterizing disease progression.

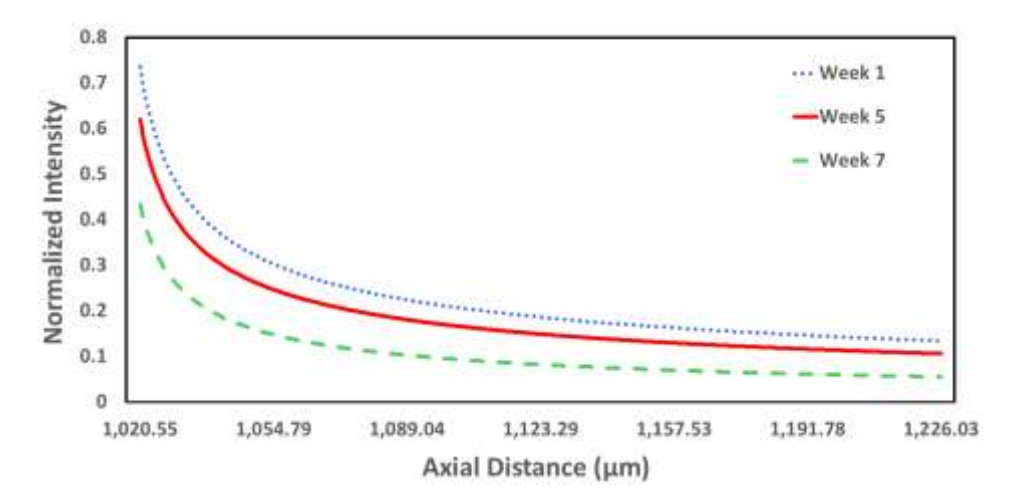


Figure 4. Averaged axial OCT intensity profiles for healthy-infected (week 1), partially healthy (week 5), and fully infected (week 7) tissue regions, illustrating progressive internal structural degradation due to bitter rot.

3.3. Volumetric Analysis

To validate the structural degradation seen in Figure 4, a three dimension (3D) analysis was conducted using MATLAB and a custom algorithm to process OCT sequences from weeks 1, 5, and 7. Volumetric reconstructions were created by stacking 2D-OCT images along the Z-axis with XY alignment. Cross-sectional XZ views within a 100 μ m depth were analyzed to assess structural changes over time. Canny edge detection highlighted tissue boundaries and morphological disruptions, revealing progressive degradation. Figure 5 presents comparative 3D visualizations of these changes across the infection stages.

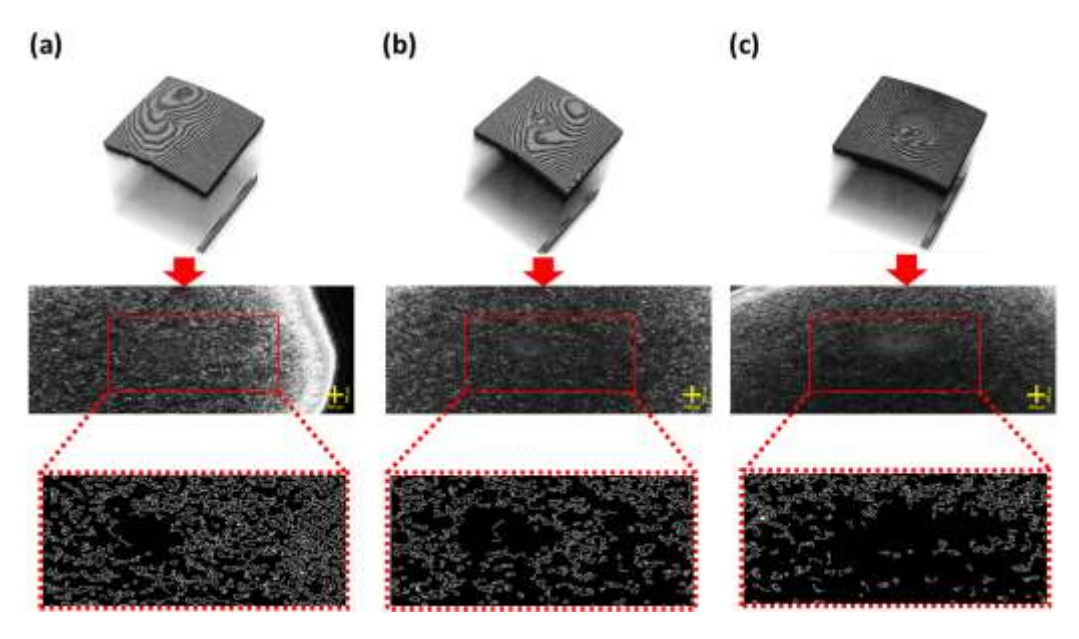


Figure 5. 3D OCT reconstructions showing internal tissue degradation due to bitter rot over time: (a) week 1 (healthy-infected), (b) week 5 (partially infected), and (c) week 7 (fully infected). XZ images within a 100 μ m depth range were used to analyze structural changes.

3.4. Irregular Oval-Shaped Pattern Progression

Three-dimensional OCT analysis revealed that irregular, oval-shaped tissue patterns emerged as key structural markers of bitter rot progression. Absent in the early stage (week 1), these patterns became faintly visible by the mid-stage (week 5) and distinctly defined by the late stage (week 7), with greater sharpness and contrast across all examined

depths (250 μ m, 500 μ m, 1000 μ m). Their spatial growth, as shown in Figure 6, reflects increasing tissue disintegration and highlights OCT's ability to capture infection-related structural changes across depth and time.

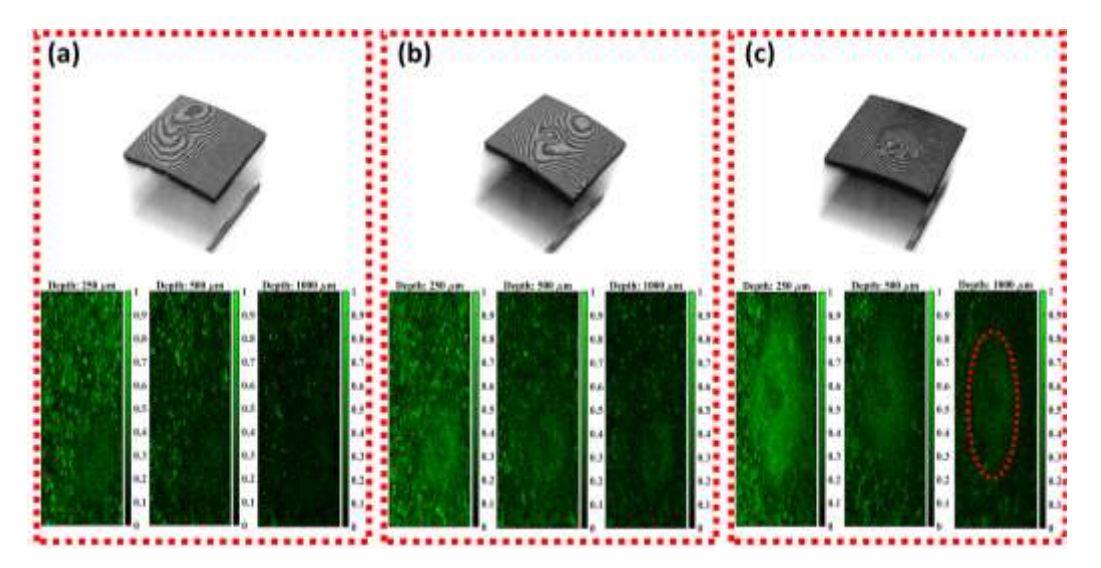


Figure 6. Structural visualization of specimen tissue at three depth levels (250 μ m, 500 μ m, and 1000 μ m) across different stages of bitter rot progression: (a) week 1 (healthy-infected); (b) week 5 (intermediate infection); (c) week 7 (fully infected). The dashed red oval overlays highlight the emergence and expansion of irregular oval-shaped tissue patterns in the infected regions, which become increasingly distinct with disease severity.

3.5. Depth-Resolved Quantification of Bitter Rot Progression Using OCT Imaging

The progression of bitter rot disease was analyzed using depth-resolved OCT imaging and a customized MATLAB program, focusing on pixel intensity distribution of irregular, oval-patterned tissues across micrometer-scale depths. Five time points (weeks 1, 2, 5, 6, and 7) were assessed using consistent ROIs defined by pre-applied masks to ensure comparability. Early stages (weeks 1–2) showed low, stable levels of threshold-passing pixels, indicating intact structure. By weeks 5–6, pixel distribution became non-uniform, signaling emerging structural anomalies. Week 7 revealed a marked increase in threshold-passing pixels, especially centrally, indicating advanced tissue degradation. As shown in Figure 7, OCT proves highly effective in quantifying internal damage, supporting early detection and monitoring in agricultural pathology.

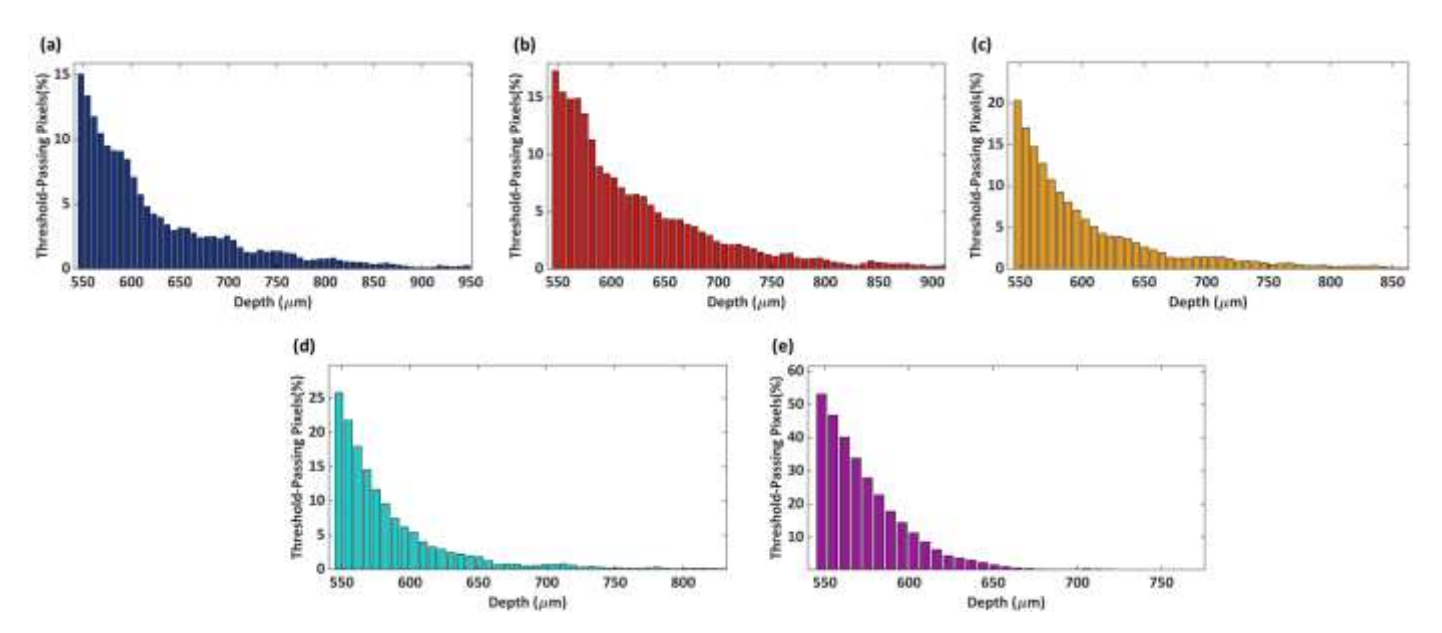


Figure 7. Depth-resolved bar plots showing the percentage of threshold-passing pixels in specimens affected by bitter rot at five time points: (a) week 1, (b) week 2, (c) week 5, (d) week 6, and (e) week 7

4. Discussion

This study demonstrates the effectiveness of OCT as a non-invasive, high-resolution imaging modality for the detection and monitoring of bitter rot disease in fruit tissue compared to other traditional methods. By utilizing micrometer-scale resolution and depthresolved imaging, OCT enabled accurate visualization of internal morphological changes without damaging the specimen. A key outcome of this work was the identification of irregular, oval-shaped tissue patterns as distinct morphological biomarkers for disease staging without damaging to specimens. These structures were absent in the healthy-infected stage, began emerging in intermediate infection, and became sharply defined in fully infected specimens, particularly at shallow imaging depths. Their clear visual distinctiveness and repeatability across samples establish them as reliable indicators of disease progression. In addition to qualitative observation, this research developed a depthresolved quantitative framework for assessing infection severity. This was achieved through pixel intensity thresholding to detect changes in structural integrity over time. Early stages exhibited a consistently low proportion of threshold-passing pixels, reflecting minimal structural degradation. In contrast, advanced stages showed a sharp and localized increase in these pixels, especially in central tissue regions, correlating with severe internal breakdown. This quantification method allowed consistent classification of samples into three clearly defined categories: healthy-infected, partially healthy, and fully infected. Such objective staging enhances repeatability and reduces reliance on subjective visual assessment.

A notable strength of the proposed method is its ability to classify disease stages solely based on OCT-derived morphological and quantitative features, eliminating the need for destructive sampling. This makes the approach highly suitable for rapid, real-time agricultural diagnostics. The reproducibility of both the morphological biomarkers and the quantitative pixel thresholding across multiple observation weeks further reinforces their robustness and diagnostic reliability. While this work focused on bitter rot, the framework's combination of axial profiling, pixel-based quantification, and volumetric reconstruction can be adapted to other plant diseases that cause tissue structure alterations. This versatility, with proven capability to monitor change through time, positions the method as a valuable tool for precision agriculture and post-harvest quality assurance.

This effort lays a solid basis for the future development of OCT as a field-portable, automated device from its current lab-based diagnostics background. Future development must incorporate adaptive refractive index calibration, dynamic region of interest selection, and machine learning integration to further enhance automation and scalability. With these enhancements, the proposed approach could be implemented in compact OCT devices capable of providing rapid, accurate, and non-destructive disease detection in agricultural settings, supporting sustainable crop management and reducing post-harvest losses.

5. Conclusions

This study establishes optical coherence tomography (OCT) as a powerful non-destructive imaging tool for the detection and staging of bitter rot in fruit, offering a significant advancement over conventional invasive techniques. By achieving micrometer-scale, depth-resolved imaging, OCT enabled precise classification of tissue health without compromising specimen integrity. The emergence and progression of irregular oval-shaped patterns were identified as reliable morphological biomarkers, and depth-resolved pixel analysis provided a robust quantitative measure of structural degradation. Three-dimensional reconstructions further revealed the spatial dynamics of disease evolution. These findings confirm that OCT can not only detect bitter rot at early stages but also track its progression with high accuracy. The approach's scalability, real-time potential, and adaptability to other plant diseases make it a promising candidate for integration into precision agriculture systems. Future work should prioritize automation through algorithmic refinement, adaptive refractive index calibration, and machine learning integration, enabling portable, field-deployable solutions for global post-harvest disease management.

Supplementary Materials: The following supporting information can be downloaded at: https://www.mdpi.com/article/doi/s1, Figure S1. Graphical representation of OCT intensity profile extraction along both axial and lateral directions.

Author Contributions: Conceptualization, A.D.K.; methodology, A.D.K.; software, A.D.K.; validation, N.S.K.; formal analysis, N.D.; resources, R.E.W.; writing—original draft preparation, A.D.K.; writing—review and editing, N.S.K. and N.D.; visualization, B.N.S. and M.J.; supervision, R.E.W.; project administration, J.K.; funding acquisition, U.W. All authors have read and agreed to the published version of the manuscript.

Funding: This research was supported by the Science and Technology Human Resource Development Project, Ministry of Education, Sri Lanka, funded by the Asian Development Bank (Grant No. STHRD/CRG/R3/SJ/07) research grant funded by the University of Sri Jayewardenepura, Sri Lanka (Grant No: ASP/01/RE/ENG/2022/86), and research grants funded by the Sri Lanka Institute of Information Technology, Sri Lanka (Grant Nos. PVC(R&I)RG/2025/15 and PVC(R&I)RG/2025/28).

Institutional Review Board Statement: Not applicable.

Informed Consent Statement: Not applicable.

Data Availability Statement: The data presented in this study are available on request from the corresponding author.

Conflicts of Interest: Authors declare no conflict of interest.

References

 González, E.; Sutton, T.B. Population Diversity within Isolates of Colletotrichum spp. Causing Glomerella Leaf Spot and Bitter Rot of Apples in Three Orchards in North Carolina. Plant Dis. 2004, 88, 1335–1340. https://doi.org/10.1094/PDIS.2004.88.12.1335.

- Saleah, S.A.; Kim, S.; Luna, J.A.; Wijesinghe, R.E.; Seong, D.; Han, S.; Kim, J.; Jeon, M. Optical Coherence Tomography as a Non-Invasive Tool for Plant Material Characterization in Agriculture: A Review. Sensors 2023, 24, 219. https://doi.org/10.3390/s24010219.
- 3. Cao, D.; Li, X.; Cao, J.; Wang, W. PCR Detection of the Three *Neofabraea* Pathogenic Species Responsible for Apple Bull's Eye Rot. *AiM* **2013**, *03*, 61–64. https://doi.org/10.4236/aim.2013.31009.
- 4. Freeman, S.; Katan, T.; Shabi, E. Characterization of *Colletotrichum* Species Responsible for Anthracnose Diseases of Various Fruits. *Plant Dis.* **1998**, *82*, 596–605. https://doi.org/10.1094/PDIS.1998.82.6.596.
- Gariépy, T.D.; Lévesque, C.A.; De Jong, S.N.; Rahe, J.E. Species Specific Identification of the Neofabraea Pathogen Complex Associated with Pome Fruits Using PCR and Multiplex DNA Amplification. *Mycol. Res.* 2003, 107, 528–536. https://doi.org/10.1017/S0953756203007810.
- 6. Freeman, S.; Rodriguez, R.J. Differentiation of Colletotrichum Species Responsible for Anthracnose of Strawberry by Arbitrarily Primed PCR. *Mycol. Res.* **1995**, *99*, 501–504. https://doi.org/10.1016/S0953-7562(09)80653-9.
- Barreiro, P.; Zheng, C.; Sun, D.-W.; Hernández-Sánchez, N.; Pérez-Sánchez, J.M.; Ruiz-Cabello, J. Non-Destructive Seed Detection in Mandarins: Comparison of Automatic Threshold Methods in FLASH and COMSPIRA MRIs. *Postharvest Biol. Technol.* 2008, 47, 189–198. https://doi.org/10.1016/j.postharvbio.2007.07.008.
- 8. Sankaran, S.; Mishra, A.; Ehsani, R.; Davis, C. A Review of Advanced Techniques for Detecting Plant Diseases. *Comput. Electron. Agric.* **2010**, 72, 1–13. https://doi.org/10.1016/j.compag.2010.02.007.
- 9. Shahin, M.A.; Tollner, E.W.; McClendon, R.W.; Arabnia, H.R. APPLE CLASSIFICATION BASED ON SURFACE BRUISES US-ING IMAGE PROCESSING AND NEURAL NETWORKS. *Trans. ASAE* **2002**, *45*, 1619–1627. https://doi.org/10.13031/2013.11047.
- 10. Huang, D.; Swanson, E.A.; Lin, C.P.; Schuman, J.S.; Stinson, W.G.; Chang, W.; Hee, M.R.; Flotte, T.; Gregory, K.; Puliafito, C.A.; et al. Optical Coherence Tomography. *Science* **1991**, 254, 1178–1181. https://doi.org/10.1126/science.1957169.
- 11. Fercher, A.F. Optical Coherence Tomography. J. Biomed. Opt. 1996, 1, 157. https://doi.org/10.1117/12.231361.
- 12. Podoleanu, A.G. Optical Coherence Tomography. J. Microsc. 2012, 247, 209–219. https://doi.org/10.1111/j.1365-2818.2012.03619.x.
- 13. Wijesinghe, R.; Lee, S.-Y.; Kim, P.; Jung, H.-Y.; Jeon, M.; Kim, J. Optical Inspection and Morphological Analysis of Diospyros Kaki Plant Leaves for the Detection of Circular Leaf Spot Disease. *Sensors* **2016**, *16*, 1282. https://doi.org/10.3390/s16081282.
- 14. MathWorks—Maker of MATLAB and Simulink. Available online: https://www.mathworks.com/ (accessed on 12 August 2025).
- Goulart, J.T.; Bassani, R.A.; Bassani, J.W.M. Application Based on the Canny Edge Detection Algorithm for Recording Contractions of Isolated Cardiac Myocytes. Comput. Biol. Med. 2017, 81, 106–110. https://doi.org/10.1016/j.compbiomed.2016.12.014.

Disclaimer/Publisher's Note: The statements, opinions and data contained in all publications are solely those of the individual author(s) and contributor(s) and not of MDPI and/or the editor(s). MDPI and/or the editor(s) disclaim responsibility for any injury to people or property resulting from any ideas, methods, instructions or products referred to in the content.